Time scales for fusion-fission and quasifission from giant dipole resonance decay

R. Butsch,* D. J. Hofman, C. P. Montoya, and P. Paul
Department of Physics, State University of New York at Stony Brook, Stony Brook, New York 11794

M. Thoennessen†
Department of Physics, State University of New York at Stony Brook, Stony Brook, New York 11794
and Oak Ridge National Laboratory, Oak Ridge, Tennessee 37831

(Received 2 April 1991)

Giant dipole resonance (GDR) γ rays in coincidence with fission fragments were measured in the reactions $^{16}O+^{208}Pb$ at 120 and 140 MeV, $^{24}Mg+^{196}Pt$ at 150 MeV, and $^{32}S+^{nat}W$ at 185 MeV. γ-ray–fission angular correlation measurements for $^{16}O+^{208}Pb$ (120 and 140 MeV) and $^{32}S+^{nat}W$ confirm the strong contribution of prescission γ rays to the total γ-ray spectrum. The data were analyzed with a modified statistical model code which includes the effects of nuclear dissipation in the fission process, γ decay at equilibrium and between saddle and scission, and the decay of the mononucleus formed in quasifission reactions. The extracted value for the nuclear friction coefficient of $\gamma=10\pm3$ at temperatures between 1 and 2 MeV is much larger than the upper limit for the ground state and indicates strongly overdamped large-scale mass motion. The extracted total fission time scale $\tau_{fiss}(\gamma=10)\simeq2.9\times10^{-19}$ s at 64 MeV excitation energy agrees with that extracted from recent neutron multiplicity experiments. A strong dependence of the GDR γ-ray yield on the target-projectile mass asymmetry is interpreted in terms of the quasifission process. γ-ray spectra and correlations could be fitted with the assumption of a GDR contribution from the mononucleus but required an arbitrary reduction of the total fission fragment excitation energy by 30 MeV. The quasifission lifetime was estimated to $\tau_{qf}=(2-9)\times10^{-20}$ s.

I. INTRODUCTION

Compelling evidence has recently been obtained from evaporation measurements of prescission charged particles [1–3] and neutron multiplicities [4–13] and, independently, from giant dipole resonance (GDR) decay studies [14,15] that the fission decay of hot nuclei is hindered, i.e., slowed down relative to the expectations of the standard statistical model. In the GDR studies the slowing down is deduced from a comparison of the fission decay branch relative to the γ-ray decay of the compound nucleus GDR which "ticks" with a characteristic time given by one classical dipole sum rule. In the neutron/charged-particles studies, the fission lifetime is compared to the number of neutrons/charged particles that are emitted by the compound nucleus before the system reaches the scission point. The slowing down of the fission process is interpreted in terms of a large-scale mass diffusion process including the effects of nuclear viscosity [16–22]. In these models the fission probability is evaluated as a function of time, flow velocity, and position, starting from the equilibrium deformation to the saddle-point configuration. Transient effects delay the buildup of the fission probability flow over the fission barrier. As pointed out by Kramers [23] the fission decay width, usually given by the Bohr-Wheeler expression [24] determined at the saddle point, is reduced by the diffusion process because the latter causes flux to be reflected back at the saddle point. This enhances the emission of particles and γ rays before the system passes through its saddle-point configuration. Furthermore, nuclear dissipation will also slow down the motion of the system on its way from the saddle point to the scission configuration, thereby increasing the decay probability of particles and γ rays between the saddle-to-scission transition. Giant dipole γ rays are emitted during the evolution from equilibrium to scission with an energy spectrum related to the increasing deformation of the system.

A different time scale is brought into the fission process when the system is not completely relaxed to the shape and mass of the compound nucleus (CN), but is trapped behind the conditional saddle in a highly deformed shape called the mononucleus [25]. The fissioning of such an intermediate system, called quasifission (or fast fission in the absence of a fission barrier), is assumed to proceed faster than the regular fission process of the CN [26–31]. However, some evidence, e.g., the fact that no asymmetries in the mass-angle correlation of the fragments are observed, indicates that some systems rotate through several cycles, leading to similar time scales for fusion fission and quasifission. It is then conceivable that a GDR excitation could be formed in the mononucleus for sufficiently long time to lead to observable GDR γ-ray decay. This offers the potential to determine some of the properties of the mononucleus including its lifetime.

It has been shown in earlier work [15] that the angular correlation between the GDR γ rays and the spin axis of the rotating fissioning system, defined by the plane determined by coincident fission fragments, is a sensitive indicator for an intermediate system that lives for several rotations. The form of the correlation as a function of γ-ray energy yields information about the GDR com-

ponents and thus the shape of the intermediate system, and about its approximate temperature. In addition, a simultaneous fit to the correlation and to the γ-ray spectrum can determine the strengths of the pre- and postscission GDR decays separately, which yield the time scale of the fission process relative to the GDR decay time.

It was demonstrated by Back *et al.* [29] that one can vary the contribution of the regular and the quasifission process by forming the same composite system in reactions of different target and projectile combinations. However, the quasifission process has never been investigated in regard to a possible presence of a GDR.

Thus the purpose of this paper is twofold: (1) We extend the previous GDR-fission correlation measurement [14] of the compound system ^{224}Th from an excitation of 64 MeV (120 MeV bombarding energy) to 82 MeV (140 MeV), in order to study the temperature effect on the CN fission process over a larger range, and to compare the GDR results for fission lifetimes to those inferred from neutron multiplicity measurements. (2) We then present measurements on Th compound systems at nearly the same excitation energy and spin formed in reactions of various target-projectile asymmetries, ^{16}O+^{208}Pb, ^{24}Mg+^{196}Pt, and ^{32}S+^{nat}W, in order to search for the GDR of the mononucleus.

II. EXPERIMENTAL PROCEDURE

In the experiments, beams of ^{16}O, ^{24}Mg, and ^{32}S from the Stony Brook LINAC were incident on targets of ^{208}Pb, ^{196}Pt, and ^{nat}W, respectively, producing systems with properties listed in Table I. γ-ray energy spectra in coincidence with fission fragments were recorded in a shielded 25.4×38.1-cm cylindrical NaI(Tl) detector placed at 90° to the beam direction. Four silicon surface-barrier detectors were configured in a plane 90° to the beam with one pair perpendicular to, and the other collinear with, the NaI detector axis. This permits the measurement of coincident γ rays emitted parallel (0°) and perpendicular (90°) to the compound nucleus spin axis. The ratio of these yields, $W(0°,E_\gamma)/W(90°,E_\gamma)$, is the γ-ray energy-dependent angular anisotropy which is a sensitive indicator for the presence of the GDR of a deformed long-lived nuclear system [15]. A detailed description of the experimental setup, calibration procedures, extraction of γ-ray energy spectra, and the GDR γ-ray–fission angular correlation can be found in earlier publications [15,32,33].

TABLE I. Summary of measured reactions. The columns contain the reaction, the compound nucleus (CN), the beam energy (MeV), the excitation energy (MeV) corrected for energy loss in the target, and the maximum angular momentum ($\hbar$).

Reaction	CN	E_{beam}	E^*_{CN}	J_{max}
^{16}O+^{208}Pb	^{224}Th	100[a]	44	45
		120	64	56
		140	90	75
^{24}Mg+^{196}Pt	^{220}Th	150	70	58
^{32}S+^{nat}W	~^{216}Th	185	72	57

[a]At 100 MeV only multiplicity gated singles γ-ray spectra and no γ-fission coincidences were recorded [14].

III. EXPERIMENTAL RESULTS

Since fission overwhelmingly dominates the decay of the Th composite system the γ-ray spectra should reflect the predominance of postscission γ rays emitted from the highly excited fission fragments, including γ rays associated with the decay of the GDR built on highly excited states of the fission fragments. In particular, one does not expect *a priori* to observe the γ-ray decay from the GDR of the CN. However, matching earlier observations in γ-ray singles energy spectra [14], the γ-ray spectrum in coincidence with fission fragments in the ^{16}O+^{208}Pb reaction shows the typical distinct bump around 11 MeV where the GDR of the CN is expected. This is an immediate indication of the presence of a prescission GDR in hot thorium systems [14]. In the present work these measurements were extended to 140 MeV bombarding energy, in coincidence with fission fragments, and including the determination of the γ-ray–fission fragment angular anisotropy. Figures 1(a) and 1(b) show the coincidence γ-ray energy spectra for 120 and 140 MeV in a representation which differs from the usual one. To bring out the enhanced contribution from the prescission CN GDR the experimental γ-ray spectra have been subtracted from the predicted spectra computed with the standard statistical decay of the thori-

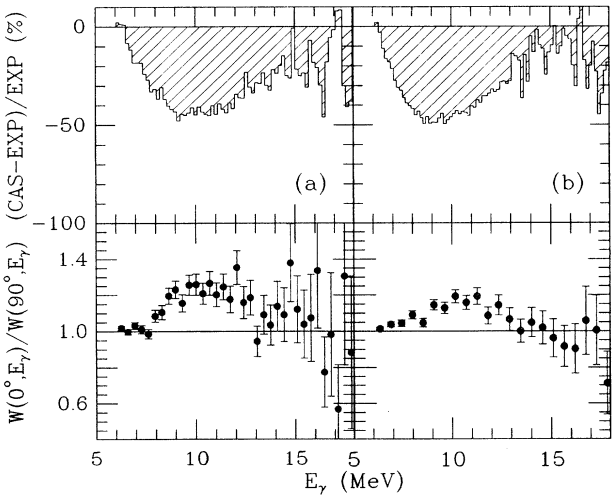

FIG. 1. Difference spectra (top) between the calculated spectra and the measured γ-ray spectra (normalized to the experiment) for the reaction ^{16}O+^{208}Pb at 120 MeV (a) and 140 MeV (b). The calculations were performed using standard statistical model parameters for the decay of the thorium compound nucleus including regular GDR, particle, and fission competition, but without dissipation effects. The bottom part shows the angular anisotropy as a function of γ-ray energy.

um compound nucleus including regular GDR, particle, and fission decay. These calculations have been performed with a modified version [15] of CASCADE [34] with parameters described elsewhere [14]. Clearly, the standard statistical model *underpredicts* the yield of high-energy γ rays in the region of the CN GDR, thus demonstrating a stronger than expected presence of the GDR of the prescission system. Even more convincing evidence for prescission GDR decay comes from the γ-ray–fission angular correlation depicted in the bottom panels of Fig. 1. They show the characteristic pattern for a GDR γ-ray decay in fissile systems with the appropriate width and position of the lower GDR component in a deformed hot CN [15]. Thus, it is evident that these hot thorium compound systems formed in the $^{16}O+^{208}Pb$ reaction live long enough to establish a GDR before the system fissions, allowing therefore a determination of the fission time scale.

The pattern observed in Fig. 1 changes significantly for the $^{32}S+^{nat}W$ reaction whose γ-ray spectrum is shown in Fig. 2(a) in the same representation as Fig. 1. Using the same standard statistical model parameters as for the 120-MeV $^{16}O+^{208}Pb$ reaction the calculations now *overpredict* the yield of γ rays in the CN-GDR region, indicating a reduced presence of the GDR. However, the "correlation bump" persists [Fig. 2(b)], indicating that a "long-lived" intermediate system is responsible for the emission of GDR-like γ rays. To investigate this surprising behavior an additional measurement was performed using the $^{24}Mg+^{196}Pt$ reaction which has a target-projectile mass asymmetry between the two other reactions. Figure 3 summarizes the γ-ray spectra in coincidence with fission fragments observed in the reactions 120-MeV $^{16}O+^{208}Pb$ (solid), 150-MeV $^{24}Mg+^{196}Pt$ (dotted), and 185-MeV $^{32}S+^{nat}W$ (dashed). The energies were chosen so that the three reactions produce thorium compound systems at nearly the same excitation energy and angular momenta (see Table I). The data are normalized to each other at $E_\gamma = 6$–7 MeV to bring out the relative strengths in the energy region of the compound nucleus GDR ($E_\gamma \approx 8$–15 MeV). The spectra exhibit a systematically decreasing presence of GDR γ rays as the projectile mass increases and the CN becomes lighter. *A priori,* one does not expect a drastic change in the γ-ray spectral shape since nearly the same compound nuclei were formed with almost identical excitation energy and maximum angular momentum. It is easy to establish with the statistical model that the small decrease in neutron number ($N=134$ for $^{16}O+^{208}Pb$, $N\sim126$ for $^{32}S+^{nat}W$) and, thus, a small increase in the fissility of the various compound systems cannot be responsible for the observed spectral changes. Rather, the difference suggests a change in reaction mechanism. It has been previously reported that in the 177-MeV $^{32}S+^{182}W$ reaction approximately 50% of the capture cross section is due to quasifission [31]. This possibility will be explored more fully in a later section.

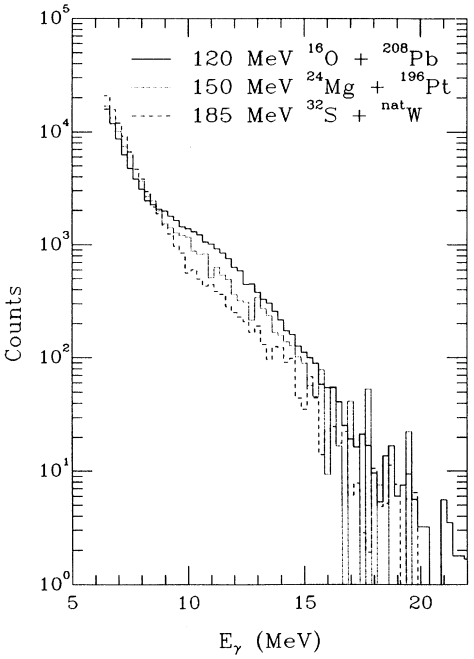

FIG. 3. γ-ray spectra of the three reactions $^{16}O+^{208}Pb$ at 120 MeV (solid), $^{24}Mg+^{196}Pt$ at 150 MeV (dotted), and $^{32}S+^{nat}W$ at 185 MeV (dashed). The spectra were normalized to each other between 6 and 7 MeV.

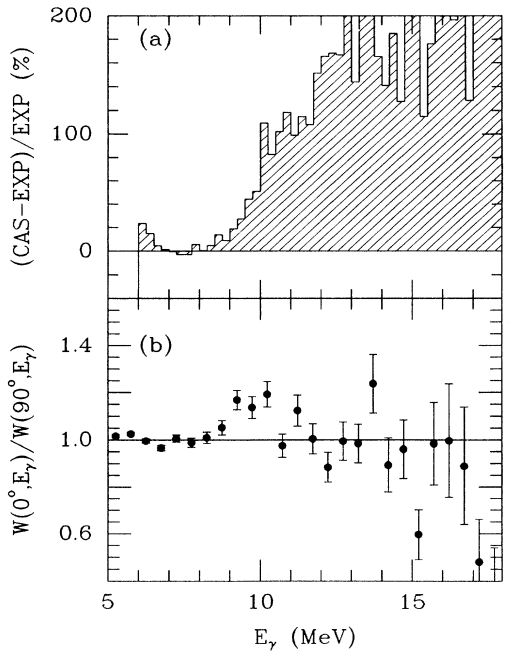

FIG. 2. Same as Fig. 1 for the reaction $^{32}S+^{nat}W$ at 185 MeV.

IV. STATISTICAL MODEL ANALYSIS INCLUDING DISSIPATION

This section outlines further modifications to the statistical model code CASCADE [34] that had been previous-

ly modified to include the statistical decay of excited fission fragments [15]. The relevant equations for particle decay (neutron, proton, alpha), γ-ray decay including the decay of the GDR and fission without nuclear dissipation have been summarized elsewhere [32]. Here, we will describe additional ingredients which account for the effects of nuclear dissipation in the fission degree of freedom. From these a fission time scale will be derived.

Following Refs. [16–21] we consider the fission process at three different stages of evolution: (1) the buildup of the fission motion in the potential minimum; (2) the movement over the barrier; and (3) the motion from the saddle to the scission point.

We assume that particle and γ-ray decay start with their full decay widths at time $t=0$, when the compound nucleus is formed at the equilibrium deformation. The buildup of the fission motion, however, occurs with a time constant τ_f due to transient effects that have their origin in the coupling of the collective fission degrees of freedom to nucleonic excitations. We describe this by a time-dependent fission decay width at the saddle point:

$$\Gamma_f(t)=\Gamma_f^0[1-\exp(-t/\tau_f)] ,$$

where τ_f can be viewed as a delay time for the fission probability flow to reach the saddle point. This fission delay leads to a relatively enhanced particle and γ-ray emission while the nucleus is near the equilibrium configuration.

As the fission motion reaches the saddle point the viscous diffusion process results in a reduction of the normal fission width, as was recognized by Kramers [23]. Using the Bohr-Wheeler expression for the normal, nondissipative, fission width, Kramers' solution is given by

$$\Gamma_f^{\text{Kramers}}=\Gamma_f^{\text{BW}}(\sqrt{1+\gamma^2}-\gamma) ,$$

with the nuclear friction coefficient $\gamma=\beta/2\omega_0$. β denotes the reduced dissipation coefficient [17,18] and ω_0 describes the potential curvature at the fission saddle point.

Identifying Γ_f^0 with the Kramers width we obtain a modified fission decay width to be used in the CASCADE calculations of

$$\Gamma_f(t)=\Gamma_f^{\text{Kramers}}[1-\exp(-t/\tau_f)] . \quad (1)$$

One would expect that nuclear dissipation will affect all large-amplitude nuclear collective motions, i.e., not only fission, but also the collective vibration of protons versus neutrons inside the nucleus which manifests itself in the decay of the giant dipole resonance. Recent observations, however, of the prescission GDR decay in hot, fissile nuclei [14,15] indicate that the GDR energy and γ transition strength, empirically one classical dipole sum rule, are not affected by nuclear dissipation mechanisms. This may be explained within the model of nuclear elastoplasticity proposed by Nörenberg [35].

Nuclear dissipation also slows down the fission motion from the saddle to the scission point. As it was shown by Hofman and Nix [36], the saddle-to-scission time, including dissipation, τ_{ssc}, may be approximated by

$$\tau_{\text{ssc}}=\tau_{\text{ssc}}^0(\sqrt{1+\gamma^2}+\gamma) , \quad (2)$$

with τ_{ssc}^0 being the time without dissipation. (For the reactions under consideration τ_{ssc}^0 can be calculated to be [37] $\tau_{\text{ssc}}^0\approx 3\times 10^{-21}$ s.) Thus, for a large saddle-to-scission time scale, particle and γ-ray emission may be enhanced further before the nucleus scissions. Thus viscosity introduces three additional parameters into the statistical model calculations: the dimensionless friction coefficient γ, the fission delay time τ_f, and the saddle-to-scission time τ_{ssc}.

Whereas enhanced neutron emission has been analyzed [6,13] in terms of the two time constants τ_f and τ_{ssc}, we elect to analyze our data in terms of the friction constant γ. This requires a relationship between τ_f and γ. In the limit of overdamped motion ($\beta\gg 2\omega_1$) the relation between τ_f and the reduced nuclear dissipation coefficient β may be taken as [17]

$$\tau_f=\frac{\beta}{2\omega_1^2}\ln(10B_f/T) , \quad (3)$$

with ω_1 being the assault frequency, B_f the height of the fission barrier, and T the nuclear temperature. For underdamped motion ($\beta\ll 2\omega_1$) τ_f is given by

$$\tau_f=\frac{1}{\beta}\ln(10B_f/T) .$$

Since $\omega_1\approx\omega_0$ we use $\omega_0=\omega_1\simeq 1\times 10^{21}\ \text{s}^{-1}$ to compute the fission delay time and the saddle-to-scission time from γ, B_f, and T. Thus, the parameter set $(\gamma,\tau_f,\tau_{\text{ssc}})$ contains only one independent parameter, γ.

The effects just described were included in CASCADE as follows. Starting with a given excitation energy E_i^* of the CN, determined by the projectile energy and ground-state Q values, the partial decay widths for each decay channel k, $\Gamma_k(E_i^*,J_i)$, summed over all final states that are allowed by the transferred angular momentum and kinetic energy of the emitted "particles" (neutron, proton, alpha, γ ray, fission), were calculated for each spin value J_i of the initial CN spin distribution. For each "box" (E_i^*,J_i) a lifetime for this first decay step was calculated from $\tau_k(E_i^*,J_i)=\hbar/\Gamma_k(E_i^*,J_i)$. Since neutron evaporation dominates completely the particle decay, the neutron lifetime was used to calculate the elapsed time (τ_{elaps}) and to describe the time evolution of the decaying system. For the decay of the initial compound nucleus population, (τ_{elaps}) is zero; therefore, the time t in the argument of the exponential in Eq. (1) is given by the neutron lifetime $\tau_n(E_i^*,J_i)$ for each initial (E_i^*,J_i) configuration. This time was then used to calculate the fission decay width for fission of the original CN for each (E_i^*,J_i) combination.

Having determined the decay of the initial CN population, an average lifetime for each decay channel k, weighted with the fusion population cross section, $\sigma^{\text{fus}}(E_i^*,J_i)$, was calculated from the average partial decay width by using

$$\Gamma_k=\frac{\sum_{E_i^*}\sum_{J_i}\Gamma_k(E_i^*,J_i)\sigma^{\text{fus}}(E_i^*,J_i)}{\sum_{E_i^*}\sum_{J_i}\sigma^{\text{fus}}(E_i^*,J_i)} . \quad (4)$$

Again, the average time to populate the "daughter" nucleus after particle and γ-ray decay is given by the average neutron lifetime $\tau_n = \hbar/\Gamma_n$. This time plus the time $\tau_n(E^*,J)$ calculated from the decay of the daughter population is now used as the elapsed time $\tau_{\rm elaps}$ for each (E^*,J) box in the daughter population to calculate the fission decay width in the daughter nucleus, etc.

During the complete decay of the compound system at equilibrium deformation, at each decay step, and for each (E^*,J) combination, the corresponding fission populations at the saddle-point configuration are created for the fission of the initial compound nucleus and of each daughter nucleus. In addition, all particle and γ-ray spectra were calculated during equilibrium decay. We shall refer to the associated γ-ray spectrum as the presaddle γ-ray spectrum.

These fission populations for each fissioning nucleus were then used to calculate the additional statistical decay of particles and γ rays during the saddle-to-scission motion. We note that, at this point, the nucleus is already committed to fission. Therefore, fission competition was excluded during the saddle-to-scission decay. To this end, a new CASCADE decay structure was calculated for each fissioning nucleus. The fission population of a particular fissioning nucleus was then used as a new "compound nucleus" population and the statistical decay of that nucleus was calculated.

To determine the appropriate excitation energy for the particle and γ-ray decay during saddle-to-scission transition, and thus the appropriate level densities, we evaluated the thermal excitation energies at the saddle and scission points according to

$$\begin{aligned} U_{\rm saddle} &= E^*_{\rm CN} - B_f - E_{{\rm rot},s} \ , \\ U_{\rm scission} &= E^*_{\rm CN} + Q_f - {\rm TKE} - E_{\rm rot,sc} - E_{\rm def} \ . \end{aligned} \tag{5}$$

The various quantities are $E^*_{\rm CN}$, the excitation energy of the compound nucleus; B_f, the fission barrier height, calculated at the mean spin of the fusion spin distribution according to the finite-range liquid drop model [38]; $E_{{\rm rot},s}$, the rotational energy of the complex at the saddle point, calculated for the mean spin of the fusion spin distribution using moments of inertia according to the finite-range liquid drop model [38]; Q_f, the fission Q value determined by the difference in binding energies from both fragments (assuming symmetric fission) and the compound nucleus; TKE, the total-kinetic-energy release in fission according to the Viola systematic [39]; $E_{\rm rot,sc}$, the rotational energy corresponding to fragment spins that were determined by parametrizing [15] the results from Schmitt *et al.* [40]; and $E_{\rm def}$, the deformation energy bound in fragment deformation and taken to be 12 MeV [31]. The excitation energy of the fission population for the saddle-to-scission decay was then determined from the average value $0.5\,(U_{\rm saddle}+U_{\rm scission})$ [13].

At equilibrium deformation, the CN has no time restriction for its statistical decay. During the saddle-to-scission transition the decay is, however, restricted by the mean saddle-to-scission time. At each decay step j the remaining time to the scission point is $\tau^j_{\rm avail} = \tau_{\rm ssc} - \sum_{m=1}^{j-1} \langle \tau_{n,m} \rangle$ and was calculated with

$$\langle \tau_{n,j} \rangle = \frac{1}{\lambda_{n,j}} \left[1 - \frac{\lambda_{n,j}\tau^j_{\rm avail} \exp(-\lambda_{n,j}\tau^j_{\rm avail})}{1-\exp(-\lambda_{n,j}\tau^j_{\rm avail})} \right] , \tag{6}$$

where $\lambda_{n,j} = \Gamma_{n,j}/\hbar$ with $\Gamma_{n,j}$ the average neutron decay width at step j [see Eq. (4), with the weighting now of the cross section of the fission population]. Equation (6) has its origin in the definition of a mean lifetime restricted, however, by the time $\tau^j_{\rm avail}$:

$$\langle \tau_{n,j} \rangle = \frac{\int_0^{\tau^j_{\rm avail}} t \exp(-\lambda_{n,j} t)\,dt}{\int_0^{\tau^j_{\rm avail}} \exp(-\lambda_{n,j} t)\,dt} \ .$$

Because of this time restriction only that part of the cross section of the fission population is allowed to decay to a daughter nucleus that occurs within the limits of the remaining time to scission. The cross sections at a given (E^*,J) were then multiplied by a factor $1-\exp[-\tau^j_{\rm avail}\Gamma_{{\rm tot},j}(E^*,J)/\hbar]$, with $\Gamma_{{\rm tot},j}(E^*,J)$ being the total decay width at step j for a given (E^*,J) combination, to calculate the population of a daughter nucleus. The remaining cross-section population at each decay step j was stored internally. At each decay step j it was checked whether $\tau^j_{\rm avail}$ has reached zero, i.e., whether the system has reached its scission configuration. In that case, the saddle-to-scission calculation was stopped and the remaining cross-section populations for all previous decay steps were then used to create the cross-section populations for the fission fragments, including a mass and TKE distribution following the description detailed elsewhere [15]. The procedure just outlined for the saddle-to-scission decay was repeated for each fission population obtained during the equilibrium decay and yielded the energy spectra of the postsaddle particles and γ rays.

Having finished the saddle-to-scission decay of all fission populations the population of each fission fragment becomes the starting point of a new CASCADE calculation of that fragment. The sum of all particle and γ-ray spectra of all fragments yields the total postscission particle and γ-ray spectrum, respectively.

In summary, this modified version of the statistical model code CASCADE provides a time-dependent treatment of the complete decay of an excited compound nucleus including a dissipation mechanism in the fission degree of freedom, yielding presaddle, postsaddle, and postscission particle and γ-ray spectra. We emphasize that the dissipation mechanism is included with only one free parameter, γ.

V. FISSION LIFETIMES IN THE ^{16}O+^{208}Pb REACTION

In this section we analyze the data obtained in the ^{16}O+^{208}Pb reaction in order to extract the friction coefficient and a time scale for fission from the GDR decay. These can then be compared to the results obtained from other studies.

The input parameters for the statistical model analysis, such as GDR parameters for the CN and fission frag-

ments, and multiplication constants for the fission barriers, were taken from previous work [14], leaving the nuclear friction coefficient γ as the only new fit parameter. The initial calculations were performed using the level density parameter reported in Ref. [14]. However, it turned out that, for very strong damping ($\gamma \geq 10$), the high-energy slope of the calculated spectrum ($E_\gamma > 15$ MeV) cannot be reproduced since the contribution of γ rays from fission fragments is now substantially smaller than those emitted prior to scission. This can be offset by either lowering the fission barrier height or the level density parameter a for fission fragment decay, both of which would result in an increased γ-ray contribution from fission fragments. Lowering the fission barrier height increases the fission fragment γ-ray cross section without changing very much the postscission γ-ray spectral shape. Since an increased amount of prescission γ rays at the energy of the lower component of the CN GDR is needed to describe the γ-ray spectral shape and the γ-ray–fission angular correlation this solution was rejected. Thus, $a = A/10$ were used for fragment γ decay with the large viscosity case ($\gamma = 10$) and gave satisfactory fits. Using $a = A/12$ (as frequently quoted in the analysis of neutron multiplicity data [13]) improves the fit quality at the highest energies but overpredicts the fission fragment γ-ray contribution at the CN-GDR energy. The calculated spectra were normalized to the measured spectra at low γ-ray energies where the postfission contribution dominates. The normalization constants so obtained agreed within 20% with those derived from the (simultaneously measured) fission singles counts.

Figure 4 shows the fits obtained for the γ-ray spectrum in coincidence with fission fragments, and for the γ-fission angular correlation, at 140 MeV, for four values for γ: underdamped ($\gamma = 0.1$), critical damping ($\gamma = 1$), overdamped ($\gamma = 5$), and very strong damping ($\gamma = 10$). First, we note that the calculated spectrum is indeed sensitive to the viscosity. Clearly, the underdamped case ($\gamma = 0.1$) cannot account for the excess γ rays observed in the CN-GDR energy region. Strong damping with γ between 5 and 10 is required. The same result is obtained from the fits to the data at 100 and 120 MeV. Thus we conclude that, at high excitation energies, fission is strongly overdamped. Using $5 \leq \gamma \leq 10$ in Eq. (3) yields a delay time for the onset of fission of $\tau_f \simeq 1\times10^{-20}-3\times10^{-20}$ s (using $B_f = 1.8$ to 4.1 MeV for the fission barrier height at the mean spin of the fusion spin distribution, and temperatures $T = 1.3$ to 1.9 MeV for the initial compound nucleus, for the three bombarding energies), and from Eq. (2) a saddle-to-scission time of $\tau_{ssc} \simeq (3-6)\times10^{-20}$ s. The total fission time scale can be obtained from

$$\tau_{fiss} = \frac{\sum_i \tau_{elaps}(i)\sigma^{fiss}(i)}{\sum_i \sigma^{fiss}(i)} + \tau_{ssc} ,$$

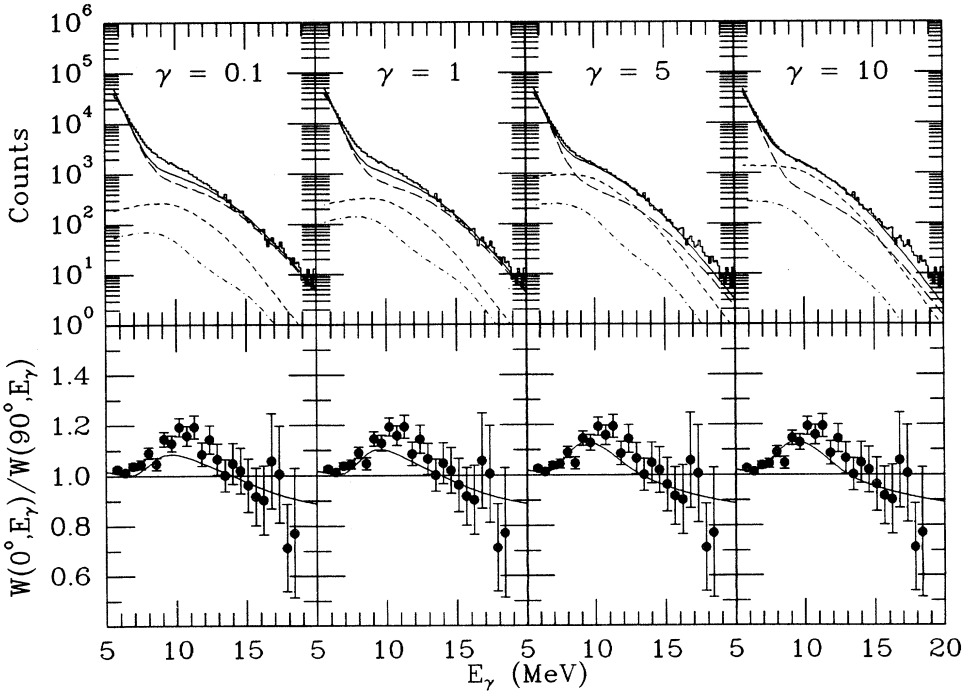

FIG. 4. γ-ray spectra (top row) and anisotropy spectra (bottom row) for the reaction $^{16}O+^{208}Pb$ at 140 MeV. The fits correspond to different values of the nuclear friction coefficient γ. The contributions to the total γ-ray spectrum (solid) are presaddle (short dashed), postsaddle (dot dashed) and postscission (long dashed). The GDR parameters for the saddle-to-scission decay were $E_1 = 9.8$ MeV, $\Gamma_1 = 3.0$ MeV and $E_2 = 15.5$ MeV, $\Gamma_2 = 5.0$ MeV.

TABLE II. Average fission times τ_{fiss}, calculated at the mean excitation energy $E_{\text{ex}}^{\text{av}}$ (in MeV), and τ_{fiss}^{1}, deduced from the fission cross section of the first step. All times are in s and are obtained for an initial excitation energy of 64 MeV for different values of the friction coefficient γ. $\gamma=0$ corresponds to calculations using standard statistical model parameters (without dissipation).

	$\gamma=0$	$\gamma=5$	$\gamma=10$
$E_{\text{ex}}^{\text{av}}$	51	48	46
τ_{fiss}	4.2×10^{-20}	3.4×10^{-19}	6.4×10^{-19}
τ_{fiss}^{1}	1.7×10^{-20}	1.2×10^{-19}	2.9×10^{-19}

TABLE III. Relative fission cross sections normalized to the fusion cross section as a function of nuclear viscosity calculated at different decay steps for 120-MeV $^{16}O+^{208}Pb$. The steps refer to consecutive daughter nuclei populated through neutron decay.

Step	$\gamma=0.1$	$\gamma=5$	$\gamma=10$
1	0.64	0.20	0.08
2	0.26	0.26	0.18
3	0.07	0.24	0.24
4	0.01	0.17	0.24
5		0.10	0.17
6		0.01	0.04

where $\tau_{\text{elaps}}(i)$ is the elapsed mean time from the beginning of the CN decay to the ith decay step up to saddle point, as described in Sec. IV. The total fission times for the 120-MeV data (initial excitation energy of 64 MeV) are listed in Table II for $\gamma=0$, 5, and 10. We note that, while the initial excitation energy is the same for the hindered and the nonhindered case, the average excitation energies are different. Averaging over six decay steps yields the different mean excitation energies $E_{\text{ex}}^{\text{av}}$ as shown in Table II. The fission time scale of the first step, i.e., at $E_{\text{ex}}=64$ MeV, can be obtained from the fraction of fission that occurs during the first step,

$$\tau_{\text{fiss}}^{1}=-\frac{\tau_{\text{elaps}}(1)}{\ln[1-\sigma_{\text{fiss}}(1)/\sigma_{\text{fiss}}^{\text{total}}]}+\tau_{\text{ssc}}\ .$$

The fission time scales τ_{fiss}^{1} at $E_{\text{ex}}=64$ MeV (Table II) are shorter than the excitation energy averaged fission times σ_{fiss}. A comparison of the fission times with and without hindrance shows that friction slows the fission process down by a factor of 8–15.

Over the range of excitation energies covered in this experiment, from 44 to 90 MeV, our fits do not show any dependence of nuclear friction on the excitation energy, within the accuracy of the procedure, i.e., of the potential-energy surface or the oscillator frequencies, and of the fission barrier height.

It is interesting to note that $\gamma=0.1$ (underdamped case) and $\gamma=5$ (overdamped case) yield exactly the same value for the fission delay time τ_f inside the saddle and thus produce comparable total fission time scales τ_{fiss}. One might at first suspect that comparable times would lead to comparable GDR γ intensities making the spectra insensitive to the viscosity. The fact that the γ-ray spectra are sensitive to the viscosity stems largely from the Kramers factor, which modifies the fission width and thus enhances γ-ray and particle emission, and which is missed if the decay multiplicities are directly analyzed in terms of time scales. Importantly, the Kramers factor does *not* change the total fission width significantly, but merely redistributes the cross section for fission from the earlier to the later decay steps. This is demonstrated in Table III, which lists the relative fission cross sections (normalized to the fusion cross section), computed with the fit parameters of Fig. 4, over the first five steps, for underdamped and overdamped cases. The case $\gamma=10$ gives a residue cross section $\sigma_{\text{res}}=19$ mb and a fission cross section $\sigma_f=1228$ mb, and $\gamma=0.1$ gives $\sigma_{\text{res}}<1$ mb and $\sigma_f=1248$ mb, which are both compatible with all available data [41]. A precision measurement of the residue cross section would clearly be desirable.

Finally, we address the question whether other than compound nuclear reaction mechanisms may contribute to the observed excess GDR γ rays in the $^{16}O+^{208}Pb$ reaction, specifically, quasifission reactions and incomplete fusion reactions. As can be concluded from the basic work of Back and collaborators [28,29] we do not expect an influence of quasifission in the $^{16}O+^{208}Pb$ reaction. However, at the highest bombarding energy of 140 MeV, corresponding to $E/A=8.8$ MeV, γ rays emerging from incomplete fusion (ICF) reactions might contribute to the observed spectrum.

To estimate the fraction of ICF to the measured fission cross section we follow the description of Morgenstern *et al.* [42]. From their Fig. 2 we extract that approximately 4% and 20% of the experimental cross section [29] of 1200 and 1500 mb are due to ICF, for 120-MeV and 140-MeV $^{16}O+^{208}Pb$, respectively. In the following, we concentrate on the highest bombarding energy and neglect ICF at 120 MeV.

According to Wilczynski's sum-rule model [43] we consider the α channel to have the strongest effect on the γ-ray spectrum. Having determined the effective laboratory energy of the "^{12}C projectile" and the corresponding ICF cross section, the angular momentum space due to ICF can be transformed into the "pseudocompound" reaction $^{12}C+^{208}Pb$. Standard CASCADE calculations (i.e., without fission hindrance) were then performed using the proper angular momentum windows for $^{16}O+^{208}Pb$ and $^{12}C+^{208}Pb$ and the resulting γ-ray spectra were added. This sum spectrum did not differ significantly from the standard compound nucleus calculations for the full angular momentum space. Thus, we conclude that ICF in the 140-MeV $^{16}O+^{208}Pb$ reaction cannot account for the excess γ rays observed in the CN-GDR energy region.

VI. COMPARISON WITH NEUTRON MULTIPLICITIES

A series of recent experiments has focused on the neutron multiplicity [11,13] to deduce fission lifetimes by comparison with the "neutron emission clock." This ap-

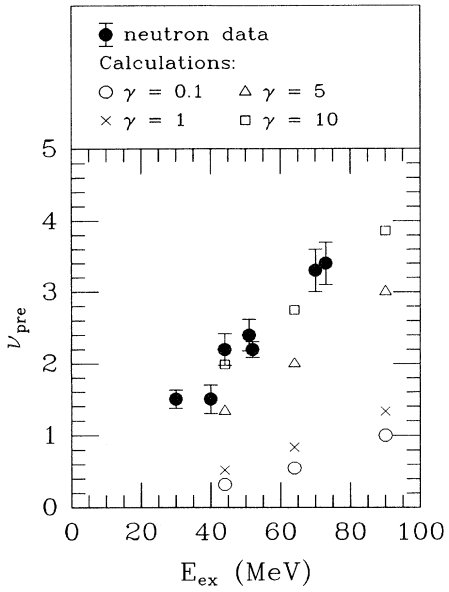

FIG. 5. Prescission neutron multiplicity as a function of excitation energy. Results from statistical model calculations with $\gamma=0.1$ (○), $\gamma=1$ (×), $\gamma=5$ (△), and $\gamma=10$ (□) are compared to experimental values (●) from Ref. [12].

proach is very similar to the one used in the present paper, and the results should be consistent.

Since in our procedure particle multiplicities are obtained along with the calculation of the γ-ray spectrum, our results also make detailed predictions about the neutron multiplicities for equilibrium decay (i.e., presaddle) and for neutrons that are emitted during the saddle-to-scission motion (postsaddle). These calculations indicate that most of the γ rays (see Fig. 4) and neutrons are emitted *before* the system reaches the saddle point. This differs significantly from some of the neutron multiplicity analyses that assumed that neutrons were predominantly emitted during the saddle-to-scission motion. Our computed multiplicities for the $^{16}O+^{208}Pb$ reaction are compared in Fig. 5 to recent neutron multiplicity measurements [12] obtained with $^{16}O+^{208}Pb$ and very similar reactions. The results obtained for a viscosity parameter $\gamma=10$ agree quantitatively with the neutron data. Viscosities of $\gamma<5$ seem to be ruled out. From the combined fits to γ-ray spectrum and neutron multiplicity we conclude that the viscosity parameter $\gamma=10\pm3$.

The quantitative success of our neutron multiplicity calculations lends support to the model assumptions that were used in the present analysis of the time evolution of the fission process and that indicates that most GDR γ rays, neutrons, and particles are emitted prior to the saddle. Our analysis explicitly includes Kramers' reduction of the fission decay width whereas Hinde *et al.* [6] use the unmodified transition state value. Since the Kramers factor considerably decreases the probability for fission (e.g., critical damping with $\gamma=1$ reduces the fission decay width to $\frac{4}{10}$ of the unmodified fission decay width), particle and γ-ray emission inside the fission saddle point is enhanced. Several additional recent experiments on the emission of charged particles [45] and complex fragments [44] support this conclusion. Thus we conclude that inclusion of the Kramer's factor into any time analysis is essential.

Some recent neutron multiplicity data obtained in coincidence with evaporation residues appear to argue against friction effects inside the fission barrier [5] since the fission probability and the neutron multiplicity associated with evaporation residues are correctly reproduced with standard statistical model parameters. On the other hand, the neutron multiplicity associated with fission is underpredicted, from which Zank *et al.* concluded that the observed excess neutrons in coincidence with fission are emitted between saddle and scission point. However, multiplicities do not provide a sensitive test for statistical model parameters since various combinations of the latter may yield approximately the same multiplicity numbers.

Finally, it is interesting that a recent experiment by the HMI group [46–48] found no dependence of the total-kinetic-energy (TKE) release in fission on the prescission neutron multiplicities. Since the TKE is assumed to be a measure of the scission configuration, this result suggests that the majority of excess particles/γ rays is indeed emitted inside the fission saddle point. This conclusion was also drawn from the fission lifetime analysis of excitation function data [49].

VII. GDR DECAY AND THE QUASIFISSION PROCESS

As was shown in Fig. 2 standard (i.e., without fission hindrance) statistical model calculations which underpredict the GDR yield observed in the $^{16}O+^{208}Pb$ reaction, overpredict the GDR decay strength of the thorium system when it is formed with the $^{32}S+^{nat}W$ reaction. Inclusion of dissipation only increases the discrepancy. The observed systematic change of the spectral shapes as the projectile mass is increased from ^{16}O to ^{24}Mg to ^{32}S (Fig. 3) is too large to be explained within the statistical decay of a fully equilibrated compound nucleus. This is because the compound systems are formed at similar excitation energies and angular momenta (Table I) and the differences in the fissilities x_{CN} are negligible (Table IV). Variations of parameters (nuclear friction coefficient γ, level densities, GDR parameters for compound nucleus and fission fragment decay) did not yield any satisfactory fits for the reaction $^{32}S+^{nat}W$.

On the other hand, the probability for the quasifission process increases rapidly as the mass asymmetry in the entrance channel decreases; specifically, a 50% quasifission contribution to the capture cross section has been determined in the $^{32}S+^{nat}W$ reaction at nearly the same excitation energy [31] of our study.

The onset of quasifission may be characterized by a mean fissility parameter [50] $x_m=\frac{2}{3}x_{CN}+\frac{1}{3}x_{eff}$, which contains the compound nucleus fissility x_{CN} and the "effective fissility" x_{eff}, which is a function of the mass and charge asymmetry of the projectile and target. These fissilities are listed in Table IV for the three reactions.

TABLE IV. The important parameters for the onset of quasifission. The compound nucleus fissility (x_{CN}), effective fissility (x_{eff}), and the mean fissility (x_m) are listed together with the quasifission spin cut (J_{qf}) and the cross sections for complete fusion (σ_{CN}) and quasifission (σ_{qf}) for the three measured systems.

Reaction	CN	x_{CN}	x_{eff}	x_m	J_{qf} ($\hbar$)	σ_{CN} (mb)	σ_{qf} (mb)
$^{16}O+^{208}Pb$[a]	^{244}Th	0.76	0.44	0.65		1250	
$^{24}Mg+^{196}Pt$	^{220}Th	0.77	0.54	0.69	53	576	200
$^{32}S+^{nat}W$	$\sim^{216}Th$	0.78	0.61	0.72	34	200	300

[a]These values correspond to a beam energy of $E_{lab}=120$ MeV.

The larger values of x_{eff} and x_m for the more symmetric reactions lead to increasing contributions of the quasifission process to the total cross section. Included in Table IV are the experimentally determined fusion-fission and quasifission cross sections for $^{16}O+^{208}Pb$ [28] and $^{32}S+^{nat}W$ [31]. The cross sections for $^{24}Mg+^{196}Pt$ were calculated using the extra push model of Ref. [25]. The quasifission contributions to the total cross section are associated with the highest partial waves in the entrance channel, above a spin J_{qf}. The values for J_{qf} listed in Table IV were obtained by matching the fusion and quasifission cross sections, assuming a triangular spin distribution of the entrance channel population.

In the following, we attempt to compute the GDR decay in the presence of the quasifission process in a simple model. First, we neglect any γ-ray and particle decay contribution from the short-lived mononucleus, i.e., above J_{qf} fission is the only decay mode. Then, the total γ-ray spectrum is the sum of CN presaddle, postsaddle, and fission fragment γ rays originating from $J<J_{qf}$, and γ rays from fission fragments following quasifission. We treat the decay of the fragments from CN fission and from quasifission exactly the same [15] (although it has been noted [51,52] that the spins in quasifission fragments may not be fully equilibrated). Using then the GDR parameters and friction coefficient from the $^{16}O+^{208}Pb$ reaction it was impossible to fit the γ-ray spectra or the angular correlations of the $^{32}S+^{nat}W$ reaction. In fact, the γ rays from the fragments alone may explain the whole γ-ray spectrum. However, the observation of an anisotropy in the fission-γ angular correlation proves that GDR γ rays are emitted from an intermediate system and not just from the fragments (which would essentially yield isotropy).

We are thus forced to consider GDR decay in the mononucleus, i.e., the intermediate system formed in the quasifission process. This may not be unreasonable, since the dissipation mechanism effective in the CN system should also slow down the quasifission process. If the intermediate system formed in quasifission stays together long enough, particles and γ rays may be emitted. Of course, the assumption of a statistical decay of the mononucleus is questionable. However, it is justified to some extent in our case by the observation of rapid energy equilibration in quasifission [30] and almost full mass equilibration in the $^{32}S+^{nat}W$ reaction [31] (implied by the almost constant average fragment mass as a function of scattering angle).

The decay of the mononucleus involves some assumptions regarding its excitation energy, lifetime, and GDR parameters. The excitation energy of the mononucleus increases continuously as the system evolves from the initial ion-ion potential to the fully reorganized system with equilibrated mass and charge (but not shape). An initial excitation energy of 38 MeV was estimated from the center-of-mass energy and the potential minimum behind the fusion barrier for the ion-ion proximity potential [53]. The final excitation energy was estimated as 75 MeV from the assumption that the fragments reseparate at a scissionlike configuration [see Sec. III, Eq. (5)]. The

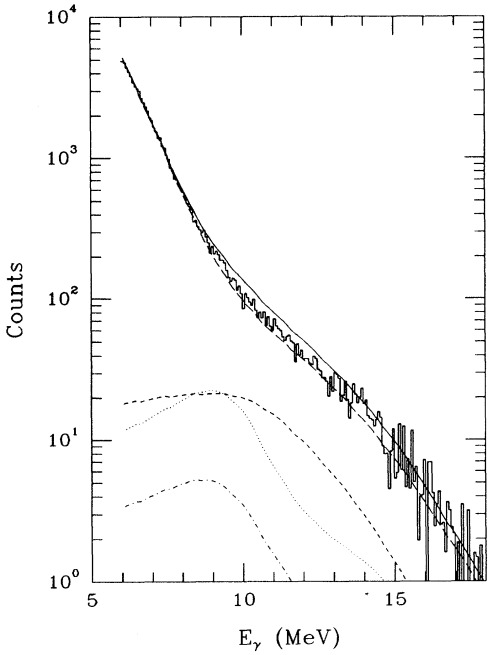

FIG. 6. Results from CASCADE calculations for the reaction $^{32}S+^{nat}W$ including statistical decay of the mononucleus. The different contributions to the total γ-ray spectrum are presaddle (short dashed), postsaddle (dot dashed), quasifission (dotted), and postscission (long dashed). The postscission calculation is a sum of the contribution following compound nucleus formation and quasifission.

value for the mean excitation energy of the mononucleus depends on the energy equilibration time and is thus not well defined.

Since the mononucleus never penetrates inside the fission barrier, its lifetime is not given by the total decay width of all possible decay channels, but is of the same nature as the saddle-to-scission time discussed in Sec. III. We introduce a quasifission lifetime (τ_{qf}) for the time from the formation of the mononucleus to its reseparation.

Although the shape of the mononucleus changes continuously during the quasifission process, theoretical calculations indicate [54] that the radial distance between the two "ion centers" does not change drastically. Thus, GDR parameters corresponding to a constant deformation larger than for the CN GDR were used. A description for the level densities was the same as for the fully equilibrated compound nucleus.

The decay of the mononucleus was then included in CASCADE as follows. For $J < J_{qf}$ the γ-ray spectra for the presaddle, postsaddle, and postscission decay were calculated for the CN as described in Sec. IV. For $J > J_{qf}$, the saddle-to-scission part of the code described in Sec. IV was used for the decay of the mononucleus, with the following minor modifications. The entrance channel population of the mononucleus was transferred immediately to the saddle-to-scission population. The saddle-to-scission lifetime τ_{ssc} is replaced by τ_{qf} and the excitation energy for the saddle-to-scission decay (Sec. IV) is now given by the average excitation energy of the mononucleus. The subsequent decay of the fission fragments was treated exactly as for the compound nucleus.

The final γ-ray spectra is then composed of five separate sources: presaddle, postsaddle, and postscission from the CN, and "postsaddle" and postscission from the mononucleus. Figure 6 shows a fit to the γ-ray spectrum of the reaction $^{32}S+^{nat}W$ and the different contributions. All CN parameters were taken from the (good) fit to $^{16}O+^{208}Pb$ data (with $a = A/8$ for the CN and the fission fragments). Initial fits started with quasifission lifetimes [30] $\tau_{qf}=2\times10^{-20}$ s and a mean excitation energy of 75 MeV, thus assuming a rapid energy equilibration, and GDR parameters for the mononucleus $E_{\parallel}=9.8$ MeV, $\Gamma_{\parallel}=2.5$ MeV and $E_{\perp}=15.5$ MeV, $\Gamma_{\perp}=5.0$ MeV, corresponding to a deformation of $\beta=0.56$. This deformation is equivalent to a radial separation of $\sim$9 fm of the quasifission system, in agreement with the closest approach of the nuclei in the ion-ion potential. No fits to the γ-ray spectrum with variations of the relevant parameters J_{qf}, τ_{qf}, and the GDR parameters could be achieved. Even adjusting the mean excitation energy of the mononucleus continuously during the decay failed. It seems not possible to describe the spectral shape as well as the anisotropy with a consistent set of parameters within this model.

However, by arbitrarily reducing the total excitation energy of the quasifission fragments by 30 MeV good fits could be obtained immediately with the parameters listed above. Figure 7 shows the fits to the γ-ray spectra from the $^{32}S+^{nat}W$ (a) and $^{24}Mg+^{196}Pt$ reactions (b). In particular, the calculations correctly yield the increasing contribution of γ rays from the mononucleus (dotted curve in Fig. 7) from the Mg to the S spectrum. We emphasize that no parameter was changed between the fit in Fig. 6 or from the $^{32}S+^{nat}W$ to the $^{24}Mg+^{196}Pt$ fits (except for using the appropriate J_{qf} values from Table IV). As in the earlier cases the normalization constants agreed within 20% with those derived from the fission singles counts.

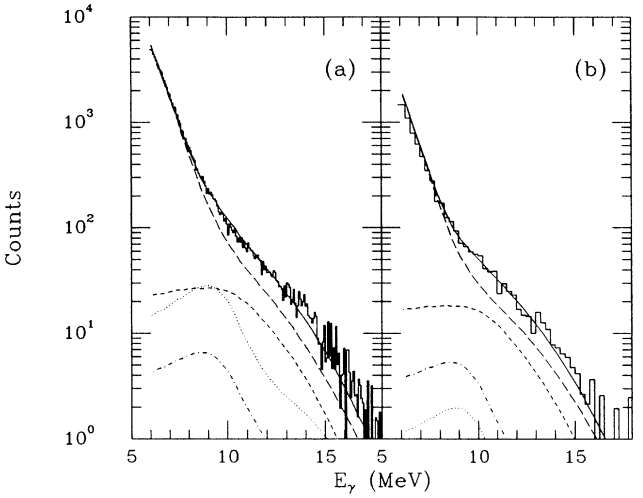

FIG. 7. Fits to the γ-ray spectra for the reactions $^{32}S+^{nat}W$ (a) and $^{24}Mg+^{196}Pt$ (b) with the parameters described in the text and the different contributions as explained in Fig. 6.

Figure 8 shows that the angular correlation calculated with the parameters from the fit to the γ-ray spectrum of

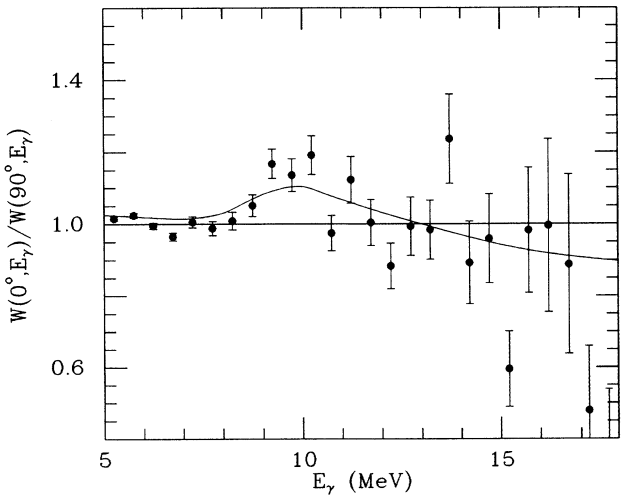

FIG. 8. Fission–γ-ray anisotropy data for the reaction $^{32}S+^{nat}W$. The solid curve was calculated using the parameters from the fits of Fig. 7.

Fig. 7 can reproduce the anisotropy around 9 MeV of the data.

A good fit with the chosen quasifission lifetime of $\tau_{qf}=2\times10^{-20}$ s requires a mean excitation energy of 75 MeV for the mononucleus. An equally good fit could be achieved with a reduced excitation energy (55 MeV) and a longer quasifission lifetime of $\tau_{qf}=9\times10^{-20}$ s. Thus, estimates of the quasifission lifetime are possible (although the reduction of the fission fragment excitation energy is not understood). We obtain a lifetime of the mononucleus $2\times10^{-20}\leq\tau_{qf}\leq9\times10^{-20}$ s which is to be compared to fusion-fission lifetimes [$3-6\times10^{-19}$ s] extracted for the $^{16}O+^{208}Pb$ reaction. Theoretical estimates [54] are $\tau_{qf}\sim10^{-20}$ s. Quasifission measurements with ^{236}U induced reactions indicate a reaction time for quasifission of mass equilibrated systems of $(1-2)\times10^{-20}$ s [30].

The necessary reduction of excitation energy in the fission fragments might be explained by a larger deformation energy stored in these fragments. Alternatively, recent experiments [51,52] suggest that the quasifission fragment spin degree of freedom is not fully equilibrated. This leads to higher spins for the more symmetric fission fragments and a decrease for the asymmetric fragments. Since the mass distribution in the $^{32}S+^{nat}W$ reaction at 185 MeV is dominated by nearly symmetric fission [31], the higher spin values are favored leading to an effectively reduced excitation energy in the fragments.

VIII. CONCLUSIONS

The present work demonstrates in an independent way the important result obtained from neutron emission data, i.e., that the fission process slows down significantly, relative to the statistical model, as the compound nucleus is heated up to moderate temperatures. The GDR γ-ray decay brings two advantageous characteristics to bear on the details of the slowing down process: (1) The "clock rate," which corresponds to one classical dipole sum rule $\approx10^{-17}$ s, is always much slower than the fission time scale, and (2) the GDR spectrum depends on the deformation of the nucleus at the time of emission. Thus the quantitative analysis of the GDR spectra shows that the GDR γ rays are mostly emitted before the system passes over the fission saddle, rather than during the path from the saddle to the scission point. Thus the fission process is already strongly slowed down as the fission flux builds up at the equilibrium deformation. A consistent treatment of the motion across the barrier using the concept of nuclear viscosity then shows the importance of including the Kramer reduction factor in the barrier penetrability. Overall, in our analysis the fission process is slowed down by a factor of about 17 in the first, hottest phase after the CN has been formed. The overall fission time scale is in the order of $(3-6)\times10^{-19}$ s.

The slowing down of the fission process enhances the emission of prescission neutrons, which is consistent with neutron multiplicity data [12]. The large fission time scale agrees also with fission times extracted from the excitation function data [49]. Increased transient times for fission are also observed in peripheral heavy-ion reactions [44] with fission hindrances of about a factor of 2 in Ac, Ra, and Fr nuclei, above excitation energies of ≈50 MeV.

It is well known [55] that the liquid-drop barrier should decrease with increasing temperature because of the reduction in the surface tension. The recent interest in the fission of hot nuclei has led to a renewed consideration of the temperature dependence of the fission barrier height and of the saddle configuration. Garcias *et al.* [56] have recently calculated the temperature- and angular-momentum-dependent fission barrier of ^{240}Pu. It indicates that B_f should decrease by 40% as T increases from 1 to 2 MeV (at constant J). Newton *et al.* [57] have incorporated a temperature-dependent fission barrier into the statistical code and discuss the various connections between a T dependence and level density parameters for the $^{19}F+^{181}Ta$ reaction near the barrier. The present analysis has used the T-independent Sierk barrier. This barrier applies to the regime where shell corrections are washed out, say, $T\approx1$ MeV. It is usually reduced by a factor 0.8 to fit experimental fission cross sections. With the inclusion of fission hindrance in the temperature regime from $T=1$ to 2 MeV we had to reduce the Sierk barrier by a factor of 0.66 to 0.60, in order not to exceed the evaporation residue cross section. This reduced barrier agrees reasonably well with the temperature and angular momentum averaged barrier of Garcias *et al.* Thus the analysis used in this work effectively includes the temperature dependence of the fission barrier.

The interesting physics of this paper is contained in the nuclear viscosity parameter γ. The result, $\gamma=10\pm3$, averaged over the temperature range between 1 and 2 MeV, corresponds to a surprisingly large viscosity, leading to strongly overdamped large-scale nuclear mass motion ($\gamma=1$ for critical damping). It should be emphasized again that our consistent fits to the data in terms of a nuclear viscosity allow one to discriminate between underdamped and overdamped motion (which lead to similar time scales). The present definition of the dimensionless parameter γ is related to the reduced nuclear dissipation coefficient β, which is used in the neutron multiplicity analyses, by $\gamma=\beta/2\omega_0$. Thus it depends on the oscillation frequency, which we took to be $\omega_0=1\times10^{21}$ s^{-1}, and the numerical value of γ is not as well determined as the experimental error would indicate. The main message of this work is that CN fission at $T=1$ to 2 MeV is strongly overdamped.

We will briefly discuss how the strong damping extracted in this work and from neutron multiplicity data compares to other types of experiments and whether it can be reconciled with general theoretical expectations. Of particular interest is the question of whether the nuclear dissipation is temperature dependent. The fact that in the present analysis the normal statistical fission had to be restored at low excitation energies in order to fit the residue cross section already indicates that the viscosity increases with temperature. This was already inferred by Dagdeviren and Weidenmüller [58] in their analysis of the viscosity in the ground-state fission of uranium where they obtain $\gamma\leq0.22$.

At low temperatures the mean-free path of the nu-

cleons is of the order of the nuclear dimensions and one-body dissipation should predominate. The so-called Wall formula [59] gives a parameter-free description of this effect, which is only weakly dependent on temperature. We use the description of Jensen *et al.* [61] to translate the Wall formula dissipation into our parameter γ. The one-body dissipation is expressed in terms of the friction parameter M_{qq}. The relation between our γ and M_{qq} is given by $\gamma = M_{qq}/2m\omega_0$, where m represents the inertia parameter. They obtain for the Wall formula in the second minimum of the fission of ^{238}U $M_{qq} = 400\hbar$, which corresponds to $\gamma \simeq 2$. A recent reanalysis of fission-fragment mean kinetic energies by Nix and Sierk [60], assuming a temperature of 2 MeV, shows that for nuclei near Th ($Z^2/A^{1/3} = 1300$) the data are compatible with 0.1–0.5 times the Wall formula dissipation, thus indicating critical to somewhat underdamped fission motion. The linear response theory with one-body dissipation of Ref. [61] yields at $T = 1$ MeV about half the Wall formula, in agreement with the kinetic-energy data. Calculations including two-body dissipation [62] predict a very small viscosity at $T = 1$ MeV, of $\gamma \approx 0.02$ ($\gamma_{\epsilon\epsilon}$ in Ref. [62] $= M_{qq}$). As one expects the two-body viscosity shows a strong temperature dependence. At $T = 2$ MeV γ has increased by a factor of 3. When reviewing these theoretical calculations it becomes clear that the value for γ extracted in this work and inferred from the neutron multiplicity data is unexpectedly large. It exceeds the Wall formula and the existent two-body dissipation calculations.

In the second part of this paper we observe the effect that the γ-ray spectra and the anisotropy for the more symmetrically formed compound systems could not be described within the statistical model with or without inclusion of dissipation. The anisotropy data strongly suggest the presence of the GDR in a long-lived system different from the CN. We take this system to be the mononucleus. However, even after inclusion of the possible decay of the mononucleus in the calculations the data could not be fitted. One might question the application of the statistical model to the mononucleus decay for the following reasons. The statistical decay of the compound nucleus is assumed to start at a time zero *after* the nucleus is fully equilibrated. In the case of the mononucleus decay, however, the statistical decay is calculated *during* equilibration. A more detailed incorporation of this effect is necessary in order to understand the data. Obviously, these questions need to be addressed further by experimental and theoretical work. In addition, the population and decay of the fission fragments following the quasifission process have to be better understand before the quasifission lifetime can be reliably extracted from the data. The present fits span the range from $\tau_{qf} = (2-9) \times 10^{-20}$ s. This agrees with schematic predictions for the evolution of the quasifission process through the mononucleus.

ACKNOWLEDGMENTS

This work was supported in part by the National Science Foundation. Oak Ridge National Laboratory is operated by Martin Marietta Energy Systems, Inc. under Contract No. DE-AC05-84OR21400 with the U.S. Department of Energy. M.T. received partial support from the Joint Institute for Heavy Ion Research, Oak Ridge.

*Present address: IBM, Route 52, Hopewell Junction, NY 12533.

†Present address: Dept. of Physics & Astronomy and National Superconducting Cyclotron Laboratory, Michigan State University, East Lansing, MI 48824.

[1] L. C. Vaz, D. Logan, E. Duek, J. M. Alexander, M. F. Rivet, M. S. Zisman, M. Kaplan, and J. W. Ball, Z. Phys. A **315**, 169 (1984).

[2] N. N. Ajitanand *et al.*, Z. Phys. A **316**, 169 (1984).

[3] L. Schad, H. Ho, G.-Y. Fan, B. Lindl, A. Pfoh, R. Wolski, and J. P. Wurm, Z. Phys. A **318**, 179 (1984).

[4] D. J. Hinde, R. J. Charity, G. S. Foote, J. R. Leigh, J. O. Newton, S. Ogaza, and A. Chatterjee, Phys. Rev. Lett. **52**, 986 (1984).

[5] W. P. Zank, D. Hilscher, G. Ingold, U. Jahnke, M. Lehmann, and H. Rossner, Phys. Rev. C **33**, 519 (1986).

[6] D. J. Hinde, R. J. Charity, G. S. Foote, J. R. Leigh, J. O. Newton, S. Ogaza, and A. Chatterjee, Nucl. Phys. **A452**, 550 (1986).

[7] A. Gavron *et al.*, Phys. Rev. C **35**, 579 (1987).

[8] D. J. Hinde, J. R. Leigh, J. J. M. Bokhorst, J. O. Newton, R. Walsh, and J. E. Boldeman, Nucl. Phys. **A472**, 318 (1987).

[9] J. O. Newton, D. J. Hinde, R. J. Charity, J. R. Leigh, J. J. M. Bokhorst, A. Chatterjee, G. S. Foote, and S. Ogaza, Nucl. Phys. **A483**, 126 (1988).

[10] D. J. Hinde, H. Ogata, M. Tanaka, T. Shimoda, N. Takahashi, A. Shinohara, S. Wakamatsu, K. Katori, and H. Okamura, Phys. Rev. C **37**, 2923 (1988).

[11] D. Hilscher, H. Rossner, B. Cramer, B. Gebauer, U. Jahnke, M. Lehmann, E. Schwinn, M. Wilpert, Th. Wilpert, H. Frobeen, E. Mordhorst, and W. Scobel, Phys. Rev. Lett. **62**, 1099 (1989).

[12] D. J. Hinde, D. Hilscher, and H. Rossner, Nucl. Phys. **A502**, 497c (1989).

[13] D. J. Hinde, H. Ogata, M. Tanaka, T. Shimoda, N. Takahashi, A. Shinohara, S. Wakamatsu, K. Katori, and H. Okamura, Phys. Rev. C **39**, 2268 (1989).

[14] M. Thoennessen, D. R. Chakrabarty, M. G. Herman, R. Butsch, and P. Paul, Phys. Rev. Lett. **59**, 2860 (1987).

[15] R. Butsch, M. Thoennessen, D. R. Chakrabarty, M. G. Herman, and P. Paul, Phys. Rev. C **41**, 1530 (1990).

[16] P. Grangé and H. A. Weidenmüller, Phys. Lett. **96B**, 26 (1980).

[17] P. Grangé, Li Jun-Qing, and H. A. Weidenmüller, Phys. Rev. C **27**, 2063 (1983).

[18] P. Grangé, S. Hassani, H. A. Weidenmüller, A. Gavron, J. R. Nix, and A. J. Sierk, Phys. Rev. C **34**, 209 (1986).

[19] H. A. Weidenmüller and Zhang Jing-Shang, Phys. Rev. C **29**, 879 (1984).

[20] P. Grangé, Nucl. Phys. **A428**, 37c (1984).

[21] K. H. Bhatt, P. Grangé, and B. Hiller, Phys. Rev. C **33**,

954 (1986).
[22] H. Delagrange, C. Grégoire, F. Scheuter, and Y. Abe, Z. Phys. A **323**, 437 (1986).
[23] H. A. Kramers, Physica **7**, 284 (1940).
[24] N. Bohr and J. A. Wheeler, Phys. Rev. **56**, 426 (1939).
[25] W. J. Swiatecki, Phys. Scr. **24**, 113 (1981).
[26] J. Péter, C. Ngo, F. Plasil, B. Tamain, M. Berlanger, and F. Hanappe, Nucl. Phys. **A279**, 110 (1977).
[27] J. Tōke *et al.*, Nucl. Phys. **A440**, 327 (1985).
[28] B. B. Back, Phys. Rev. C **31**, 2104 (1985).
[29] B. B. Back *et al.*, Phys. Rev. C **32**, 195 (1985).
[30] W. Q. Shen *et al.*, Phys. Rev. C **36**, 115 (1987).
[31] J. G. Keller *et al.*, Phys. Rev. C **36**, 1364 (1987).
[32] D. R. Chakrabarty, S. Sen, M. Thoennessen, N. Alamanos, P. Paul, R. Schicker, J. Stachel, and J. J. Gaardhøje, Phys. Rev. C **36**, 1886 (1987).
[33] S. Sen, D. R. Chakrabarty, P. Paul, J. Stachel, and M. Thoennessen, Nucl. Instrum. Methods **A264**, 407 (1988).
[34] F. Pühlhofer, Nucl. Phys. **A260**, 276 (1977).
[35] S. Ayik and W. Nörenberg, Z. Phys. A **309**, 121 (1982).
[36] H. Hofman and J. R. Nix, Phys. Lett. **122B**, 117 (1983).
[37] J. R. Nix, Nucl. Phys. **A130**, 241 (1969).
[38] A. J. Sierk, Phys. Rev. C **33**, 2039 (1986).
[39] V. E. Viola, K. Kwiatkowski, and M. Walker, Phys. Rev. C **31**, 1550 (1985).
[40] R. P. Schmitt, G. Mouchaty, and D. R. Haenni, Nucl. Phys. **A427**, 614 (1984).
[41] E. Vulgaris, L. Grodzins, S. G. Steadman, and R. Ledoux, Phys. Rev. C **33**, 2017 (1986).
[42] H. Morgenstern, W. Bohne, W. Galster, K. Grabisch, and A. Kyanowski, Phys. Rev. Lett. **52**, 1104 (1984).
[43] J. Wilczynski, K. Siwek-Wilczynska, J. van Driel, S. Gonggrijp, D. C. J. M. Hageman, R. V. F. Janssens, J. Lukasiak, and R. H. Siemssen, Phys. Rev. Lett. **45**, 606 (1980).
[44] E.-M. Eckert *et al.*, Phys. Rev. Lett. **64**, 2483 (1990).
[45] J. R. Leigh, private communication.
[46] H. Rossner, D. Hilscher, D. J. Hinde, B. Gebauer, M. Lehmann, M. Wilpert, and E. Mordhorst, Phys. Rev. C **40**, 2629 (1989).
[47] D. Hilscher, private communication.
[48] E. Mordhorst, M. Strecker, H. Frobeen, M. Gasthuber, W. Scobel, B. Gebauer, D. Hilscher, M. Lehmann, H. Rossner, and Th. Wilbert, Phys. Rev. C **43**, 716 (1991).
[49] J. B. Natowitz, M. Gonin, M. Gui, K. Hagel, Y. Lou, D. Utley, and R. Wada, Phys. Lett. B **247**, 242 (1990).
[50] J. Blocki, H. Feldmeier, and W. J. Swiatecki, Nucl. Phys. **A459**, 145 (1986).
[51] K. Lützenkirchen, J. V. Kratz, G. Wirth, W. Brüchle, K. Sümmerer, R. Lucas, J. Poitou, and C. Grégoire, Nucl. Phys. **A452**, 351 (1986).
[52] B. B. Back, S. Bjørnholm, T. Døssing, W. Q. Shen, K. D. Hildenbrand, A. Gobbi, and S. P. Sørensen, Phys. Rev. C **41**, 1495 (1990).
[53] J. Blocki, J. Randrup, W. J. Swiatecki, and C. F. Tsang, Ann. Phys. (N.Y.) **105**, 427 (1977).
[54] C. Grégoire, C. Ngo, E. Tomasi, B. Remaus, and F. Scheuter, Nucl. Phys. **A387**, 37c (1982).
[55] G. Sauer, H. Chandra, and U. Mosel, Nucl. Phys. **A264**, 221 (1976).
[56] F. Garcias, M. Barranco, H. S. Wio, C. Ngo, and J. Nemeth, Phys. Rev. C **40**, 1522 (1989).
[57] J. O. Newton, D. G. Popescu, and J. R. Leigh, Phys. Rev. C **42**, 1772 (1990).
[58] N. R. Dagdeviren and H. A. Weidenmüller, Phys. Lett. B **186**, 267 (1987).
[59] J. Blocki, Y. Boneh, J. R. Nix, J. Randrup, M. Robel, A. J. Sierk, and W. J. Swiatecki, Ann. Phys. (N.Y.) **113**, 330 (1978).
[60] J. R. Nix and A. J. Sierk, Los Alamos Report LA-UR-87-133, 1987.
[61] A. S. Jensen, K. Reese, H. Hofmann, and P. J. Siemens, in *Physics and Chemistry of Fission, 1979* (IAEA, Vienna, 1980), Vol. II, p. 423.
[62] E. Werner, H. S. Wio, H. Hofmann, and K. Pomorski, Z. Phys. A **299**, 231 (1981).